Single-Molecule Magnets

DOI: 10.1002/ange.201303005

# Influence of the Ligand Field on Slow Magnetization Relaxation versus Spin Crossover in Mononuclear Cobalt Complexes**

*Fatemah Habib, Oana R. Luca, Veacheslav Vieru, Muhandis Shiddiq, Ilia Korobkov, Serge I. Gorelsky, Michael K. Takase, Liviu F. Chibotaru, Stephen Hill, Robert H. Crabtree, and Muralee Murugesu**

*Dedicated to Professor George Christou on the occasion of his 60th birthday*

One hundred years ago Alfred Werner won the Nobel Prize in chemistry for his pioneering work with inorganic coordination compounds, which was mainly attributed to his work on mononuclear cobalt complexes.[1] Although this chemistry has been well-developed, in recent years it continues to reveal new and interesting magnetic properties derived from the molecular geometry of these complexes.[2] Indeed since the discovery of magnet-like behavior in a mononuclear transition-metal complex,[3] a sudden re-emergence of interest occurred in 3d molecules acting as molecular magnets.[4] This is mainly due to the fact that these model mononuclear complexes can unravel the origin of magnetic anisotropy due to their unquenched first-order orbital angular momentum.[4,5] When large uniaxial anisotropy ($D$) is coupled with the intrinsic spin ($S$) of a molecule, an anisotropic barrier ($U = S^2 | D |$) for the reversal of the magnetization can be seen.[6] Such molecules are termed single-molecule magnets (SMMs) or, for mononuclear complexes, single-ion magnets (SIMs).[4,7,8] To compensate for low-spin values in 3d ions, highly anisotropic metal ions, such as $Fe^{II}$ or $Co^{II}$, are used.[4,6c]

Moreover, 3d complexes can exhibit spin crossover (SCO) behavior.[9] For $3d^4$–$3d^7$ metal ions, high-spin (HS)–low-spin (LS) crossover can occur if the ligand field is tuned such that a balance between strong and weak field ligands is achieved.[10] Strong-field terpyridine (terpy) ligands can be ideal for isolating such systems. With this in mind we have carefully studied three related compounds based on the $Co^{II}$-terpy system where we fine-tune the ligand field by controlling the number of coordinated terpy ligands as well as the remaining terminal ligands, leading to unique magnetic properties of SIM and SCO behavior. Herein we unravel the inherent physical properties of $[Co(terpy)Cl_2]$ (**1**), $[Co(terpy)(NCS)_2]$ (**2**), and $[Co(terpy)_2](NCS)_2 \cdot 1.5\,H_2O$ (**3**) through structural, spectroscopic, computational, and magnetic studies.

The synthetic procedure and crystallographic data for the complexes are described in the Supporting Information (Tables S1–S3). In **1**, the $Co^{II}$ ion adopts $C_s$ symmetry and is elevated in respect to the plane formed by the three N atoms of the terpy ligand (N1–N3), yielding a distorted square-based pyramid (Figure 1).[11] The packing diagrams along the *a*-, *b*- and *c*-axes show antiparallel packing of $Co^{II}$ units (Supporting Information, Figures S1–S3) with the closest intermolecular distance between terpy centroids of 3.79 Å, leading to π–π stacking. In complex **2**,[12] the $Co^{II}$ coordination shifts towards trigonal bipyramidal with the $Co^{II}$ ion coordinating within the plane of the terpy ligand. The packing diagrams (Supporting Information, Figures S4–S6) indicate parallel alignment of the $Co^{II}$ units with a distance of 3.66 Å between the centroids of the terpy ligands. These solid-state interactions are strong enough to induce a change in the $Co^{II}$ geometry, which adopts $C_{2v}$ as opposed to $C_s$ symmetry. In **3**, the six-coordinate bis(terpy) complex adopts a distorted octahedral geometry (Figure 1c) and packs in a similar fashion to **1** (Supporting Information, Figures S7, S8), with an intermolecular terpy centroids distance of 3.70 Å. Unlike the weak-field chloride ligands in complex **1**, nitrogen-containing ligands of **2** and **3** are known to have stronger fields, which will have significant implications on the electronic distribution and in turn the magnetic properties of these complexes.

To probe further the electronic properties of all complexes, density functional theory (DFT) calculations were performed (see the Supporting Information). Geometry optimization of **1** resulted in a structure with $C_s$ symmetry and a HS state of $S = 3/2$, in close agreement with the X-ray data (Figure 1), while for **2**, a HS $C_s$ symmetric structure (Supporting Information, Scheme S1) was obtained. There-

[*] F. Habib, Dr. I. Korobkov, Dr. S. I. Gorelsky, Prof. M. Murugesu
Chemistry Department, University of Ottawa
D'Iorio Hall, 10 Marie Curie, Ottawa, ON, K1N6N5 (Canada)
E-mail: m.murugesu@uottawa.ca
Homepage: http://mysite.science.uottawa.ca/mmuruges/index.html

O. R. Luca, Dr. M. K. Takase, Prof. R. H. Crabtree
Chemistry Department, Yale University
P.O. Box 208107, New Haven, CT 06520 (USA)

V. Vieru, Prof. L. F. Chibotaru
Division of Quantum and Physical Chemistry and
INPAC-Institute for Nanoscale Physics and Chemistry
Katholieke Universiteit Leuven
Celestijnenlaan, 200F, 3001 Leuven (Belgium)

M. Shiddiq, Prof. S. Hill
National High Magnetic Field Laboratory and
Department of Physics, Florida State University
Tallahassee, FL 32310 (USA)

[**] We thank the University of Ottawa, NSERC, ERA, CFI, and ORF. O.R.L. and R.H.C. thank CETM for Innovative Energy Storage funded by the U.S. Department of Energy, Office of Science, and Office of Basic Energy Sciences under Award Number DE-SC00001055. Work performed at the National High Magnetic Field Laboratory was supported by the US National Science Foundation (DMR1309463 and DMR1157490) and by the State of Florida.

Supporting information for this article is available on the WWW under http://dx.doi.org/10.1002/anie.201303005.

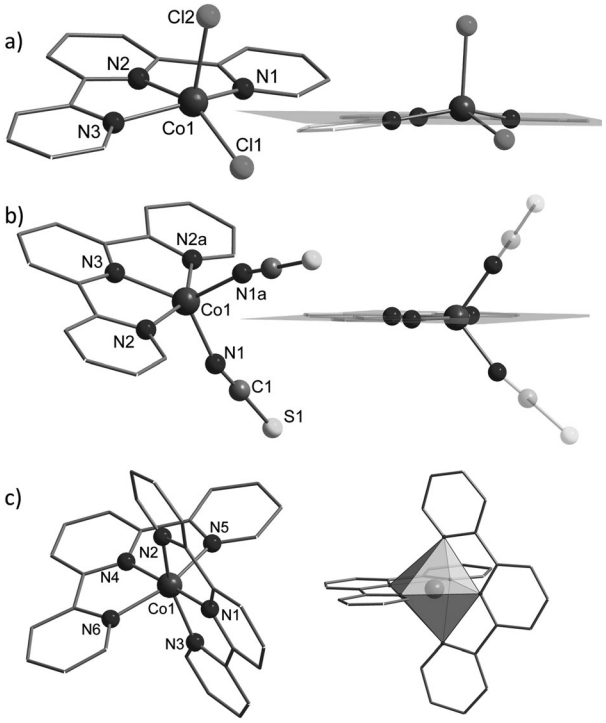


***Figure 1.*** Molecular structures of a) [Co(terpy)$Cl_2$] (**1**), b) [Co(terpy)-$(NCS)_2$] (**2**), and c) $[Co(terpy)_2]^{2+}$ (**3**). Hydrogen atoms, counterions, and solvent molecules have been omitted for clarity. The plane formed by the three N atoms of the terpy ligand (**1** and **2**) as well as the polyhedron around the $Co^{II}$ ion (**3**) are shown shaded (right).

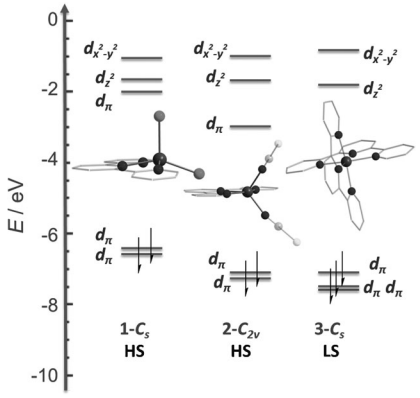


***Figure 2.*** Energy-level diagram depicting selected β-spin frontier molecular orbitals of **1** ($C_s$ symmetry), **2** ($C_{2v}$ symmetry), and **3** ($C_s$ symmetry). The increase in the number of β-spins for **3** comes at the cost of an α-spin, resulting in an overall decrease in the molecular spin state.

fore, the change from asymmetric $Co^{II}$ ($C_s$ symmetry) in solution to symmetric ($C_{2v}$ symmetry) in the solid state is likely due to the intermolecular interactions and/or the crystal packing forces. The HS state for complexes **1** and **2** can be attributed to the low coordination number of $Co^{II}$ and the relatively small difference in energy between the highest $d_\pi$ orbital and $d_{z^2}$ due to the distorted square-based pyramid geometry. The calculated metal–ligand covalency was greater in **1**, as chlorides are both σ- and π-donor ligands. Owing to interactions between the occupied π-donor orbitals of the Cl ligands and the metal $d_\pi$ orbitals, the splitting of the 3d set will be slightly smaller in complex **1** compared to complex **2** (Figure 2). TD-DFT calculations indicate that complexes **1** and **2** have low-energy ligand-field excited states with the same multiplicity as the ground state (spin quartet). The energies of the lowest-energy excited states are 0.27 eV and 0.31 eV for **1** and **2,** respectively. The presence of these low-energy excited states will affect the magnetic properties of these complexes (see below). For **3**, the orbital splitting diagram shows the three $d_\pi$ orbitals close in energy and well-separated from the two $d_\sigma$ orbitals, resulting in a low-spin complex. This LS ground state is due to the change in coordination number/geometry as well as the influence of the two strong-field terpy ligands.

In the $\chi T$ versus $T$ plot of the direct-current (dc) magnetic susceptibility measurements (Supporting Information, Figure S9), the high-temperature values are 3.34 $cm^3 K mol^{-1}$ (300 K) for **1**, 2.66 $cm^3 K mol^{-1}$ (300 K) for **2**, and 1.39 $cm^3 K mol^{-1}$ (350 K) for **3**. For **1** and **2**, the $\chi T$ products as well as curve shapes are in agreement with other experimentally observed values for a mononuclear high-spin $Co^{II}$ complex with significant anisotropy.[13,14] For **3**, the $\chi T$ curve indicates SCO behavior where the $Co^{II}$ ions show a HS–LS crossover that is completed at approximately 90 K. This change occurs gradually and begins at a temperature higher than 350 K. The low-spin value of 0.31 $cm^3 K mol^{-1}$ at 1.8 K agrees well with the theoretical value of 0.375 $cm^3 K mol^{-1}$ for a LS $Co^{II}$ ion where $S = 1/2$ and $g = 2$. The magnetization plots ($M$ versus $H$ and $M$ versus $HT^{-1}$) for **1** and **2** show non-saturation and non-superposition, respectively, of the curves at different temperatures indicating the presence of significant anisotropy (Supporting Information, Figures S10, S11) while those for **3** (Supporting Information, Figure S12) confirm the absence of anisotropy (magnetization saturates at 1.8 K and high field). The SCO behavior in **3** is a result of the added terpy ligand. The resultant change in the coordination geometry and the strong ligand-field render the LS state accessible.

The frequency dependence of the in-phase ($\chi'$) and out-of-phase magnetic susceptibility ($\chi''$) for **1** were measured under applied dc fields of 0–8.6 kOe (Supporting Information, Figure S13). As the applied field is increased, one relaxation pathway begins to appear at approximately 15–20 Hz and increases in intensity until 1.6 kOe, after which it begins to decrease. A second relaxation pathway appears between 0.1 and 1 Hz under an applied 1.2 kOe field. It appears initially as a shoulder then reaches a full peak as the applied field increases. Under applied fields of 600 Oe and 5.6 kOe (where only one relaxation pathway is clearly dominant while the other is suppressed), the $\chi''$ versus $\nu$ plots reveal clear temperature-dependent peaks down to 1.9 K (Figure 3 a). This is indicative of field-induced SMM behavior with multiple relaxation pathways, which is rather common in lanthanide-based systems but remains rare in transition-metal SIMs.[4h,15] The absence of a peak at $H = 0$ is characteristic of quantum tunneling of the magnetization (QTM), which is suppressed when a longitudinal field is applied. The anisotropic barriers (obtained by fitting this data using the

  

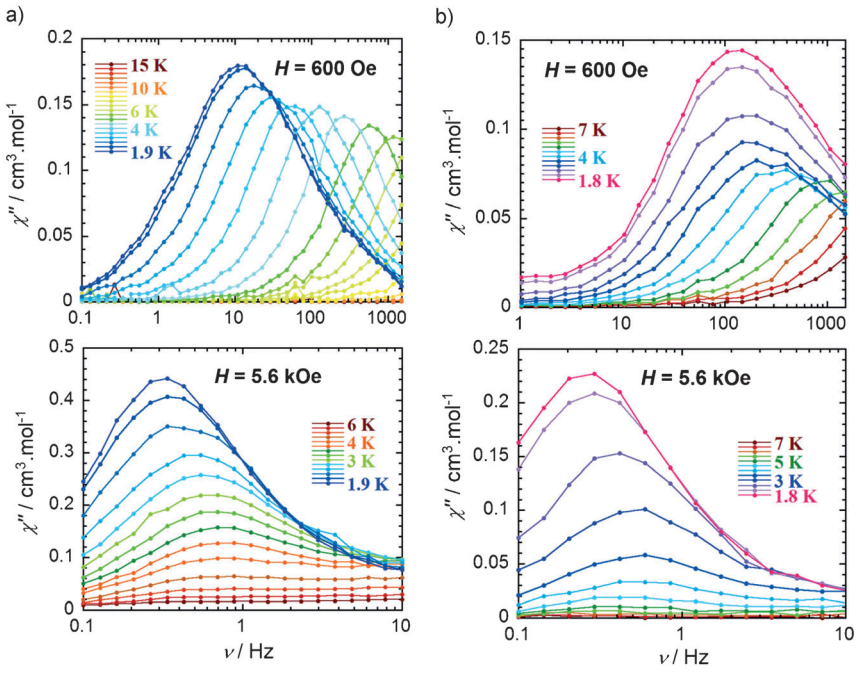


***Figure 3.*** Frequency ($\nu$) dependence of the out-of-phase magnetic susceptibility, $\chi''$, at the indicated applied fields ($H$) and temperature ranges for a) **1** and b) **2**.

Arrhenius law, $\tau = \tau_0 \exp(U_{eff}/kT)$) were calculated to be $U_{eff} =$ 28 K ($\tau_0 = 1.07 \times 10^{-6}$ s) and 4 K ($\tau_0 = 7.44 \times 10^{-2}$ s) for the fast and slow relaxation processes, respectively (Supporting Information, Figure S14). The Cole–Cole plots for both processes (Supporting Information, Figures S15, S16) yield an average $\alpha$ value of 0.20 and 0.11, respectively, indicating a fairly narrow width of relaxation times. Similar dynamic behavior is observed in **2** (Figure 3b) under the same applied dc fields as **1** with energy barriers for spin reversal of $U_{eff} =$ 17 K ($\tau_0 = 5.85 \times 10^{-6}$ s) and 3 K ($\tau_0 = 0.11$ s) for the fast and slow relaxation processes, respectively (Supporting Information, Figure S17). Owing to the absence of magnetic anisotropy (Supporting Information, Figures S9 and S12) and small spin, no slow relaxation dynamics were observed for **3**.

A surprising outcome of the DFT calculations for **1** and **2** is the large splitting between the lowest pair of occupied β-spin states and the next unoccupied levels, suggesting weak spin–orbit mixing with excited states and, hence, relatively weak anisotropy. However, making such inferences about excited states on the basis of DFT can be misleading. Therefore, ab initio calculations based on CASSCF/CASPT2/RASSI/SINGLE_ ANISO[16] were performed for **1** (Supporting Information, Tables S4–S8). These indicate strong mixing of the two lowest spin quartets by spin–orbit coupling in the first order of perturbation theory, leading to large zero-field splitting of the lowest Kramers doublets (ca. 200 $cm^{-1}$; Supporting Information, Tables S5, S6), which become quite anisotropic (Supporting Information, Table S6). However, the transversal components of the $g$ factors are still relatively large, circa 1.2–1.5, providing a possible explanation for $H = 0$ QTM via internal transverse dipolar fields. The calculated anisotropy axis lies close to the Co–Cl1 bond (Supporting Information, Figure S18, Table S8), as the ligand field exhibits higher axial character than in other directions. Fits to the magnetic data (Supporting Information, Figures S9, S19) indicate a relatively large intermolecular exchange interaction, $zJ' =$ −0.15 $cm^{-1}$, supporting the existence of π–π stacking in the crystal packing (Supporting Information, Figure S2). The large energy of the first excited Kramers doublet (ca. 200 $cm^{-1}$; Supporting Information, Table S6) shows that it cannot be associated with either barrier extracted from the ac measurements, indicating direct-type relaxation[17] where the relaxation time strongly depends on the applied dc field. For **2**, the splitting energy of the lowest Kramers doublets is about 100 $cm^{-1}$ (Supporting Information, Table S9), which is less than that seen in **1** with higher transversal components of the $g$ factor (ca. 1.7–3.0), yielding a less-anisotropic $Co^{II}$ ion. This could potentially explain the lower energy barriers observed in **2**.

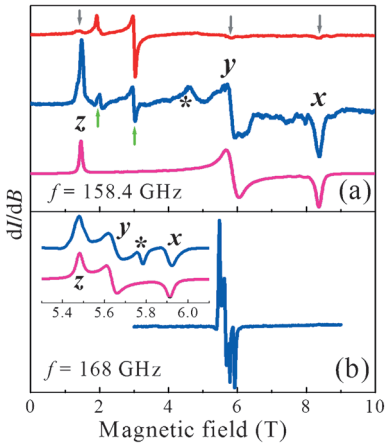


***Figure 4.*** Powder EPR spectra and simulations for complexes **1** (a) and **3** (b); Exp. 1 (blue) was performed at 2.5 K; Exp. 2 (red) was performed several months later on the same powder pellet, at 20 K. Inset: Expanded view of the spectra. Simulations (maroon) were performed using EasySpin.[18]

High-frequency EPR measurements performed on **1** and **3** are shown in Figure 4. The 158.4 GHz spectra obtained for **1** span an extremely broad field range, indicating significant magnetic anisotropy. In contrast, the 168 GHz spectrum for **3** (Figure 4b) spans a narrow range, corresponding to $g$ values of 2.03–2.19 for $S = 1/2$, that is, relatively weak anisotropy.

The first spectrum obtained for **1** (Exp. 1 in Figure 4a) is consistent with an anisotropic ground-state Kramers doublet. The three components, labeled $x$, $y$, and $z$, have similar intensities and widths, and their respective shapes suggest that they correspond to the three components of the effective $g$-

tensor of a single species, as confirmed by the effective spin $S' = 1/2$ simulation (Sim. 1) yielding $g_{eff,x} = 1.35$, $g_{eff,y} = 1.93$, and $g_{eff,z} = 7.75$. The weaker features marked by green arrows are found to dominate the spectrum obtained several months later (Exp. 2), suggesting that the sample might have formed an octahedral complex by coordinating to water molecules; the original *x*, *y*, and *z* components are barely discernible (gray arrows). Regardless, the *g*-values obtained for the pristine sample (Exp. 1) can only be associated with a HS $S = 3/2$ $Co^{II}$ species. Moreover, they suggest that the magnetic anisotropy is of the easy-axis type as predicted from the ab initio studies. For **3**, the main peaks labeled *x*, *y*, and *z* can only be due to orbitally non-degenerate LS $Co^{II}$, with $S = 1/2$ ground state. This is consistent with stronger-field terpyridine ligands as well as the distorted $O_h$ geometry (Figure 2).

In conclusion, the chemistry developed long ago by Werner continues to unveil exciting new phenomena such as those we have shown using three $Co^{II}$ complexes with varying ligand fields and geometry. Complexes **1** and **2** exibit a rare phenonmenon in transition metal SIMs of magnetization relaxation through multiple pathways. When the $Cl^-$ ligands in **1** were exchanged for $NCS^-$ ligands in **2**, the energy barrier decreased significantly. In **3**, it disappeared as the LS state became accessible at low temperature due to changes in coordination number and geometry, resulting in SCO behavior. Overall, the spin states as well as the magnetic properties studied using a combination of DFT and ab initio calculations confirm the experimentally observed properties. By tuning the ligand field strength around the metal ion as well as its geometry, it becomes possible to control the physical properties; a feat that has been consistently pursued since before the days of Werner.

Received: April 10, 2013
Published online: September 5, 2013
Publication was delayed at the author's request.

**Keywords:** cobalt · multiple relaxation pathways · single-molecule magnets · spin crossover

[1] E. C. Constable, C. E. Housecroft, *Chem. Soc. Rev.* **2013**, *42*, 1429.

[2] a) F. A. Cotton, D. M. L. Goodgame, M. Goodgame, *J. Am. Chem. Soc.* **1961**, *83*, 4690; b) G. E. Kostakisa, S. P. Perlepes, V. A. Blatov, D. M. Proserpio, A. K. Powell, *Coord. Chem. Rev.* **2012**, *256*, 1246; c) J. L. Rodríguez-López, F. Aguilera-Granja, K. Michaelian, A. Vega, *Phys. Rev. B* **2003**, *67*, 174413; d) I. A. Gass, S. Tewary, A. Nafady, N. F. Chilton, C. J. Gartshore, M. Asadi, D. W. Lupton, B. Moubaraki, A. M. Bond, J. F. Boas, S.-X. Guo, G. Rajaraman, K. S. Murray, *Inorg. Chem.* **2013**, *52*, 7557.

[3] a) S. Karasawa, G. Zhou, H. Morikawa, Noboru Koga, *J. Am. Chem. Soc.* **2003**, *125*, 13676; b) D. E. Freedman, W. H. Harman, T. D. Harris, G. J. Long, C. J. Chang, J. R. Long, *J. Am. Chem. Soc.* **2010**, *132*, 1224.

[4] a) W. H. Harman, T. D. Harris, D. E. Freedman, H. Fong, A. Chang, J. D. Rinehart, A. Ozarowski, M. T. Sougrati, F. Grandjean, G. J. Long, J. R. Long, C. J. Chang, *J. Am. Chem. Soc.* **2010**, *132*, 18115; b) T. Jurca, A. Farghal, P.-H. Lin, I. Korobkov, M. Murugesu, D. S. Richeson, *J. Am. Chem. Soc.* **2011**, *133*, 15814; c) P.-H. Lin, N. C. Smythe, S. I. Gorelsky, S. Maguire, N. J. Henson, I. Korobkov, B. L. Scott, J. C. Gordon, R. T. Baker, M. Murugesu, *J. Am. Chem. Soc.* **2011**, *133*, 15806; d) J. Vallejo, I. Castro, R. Ruiz-García, J. Cano, M. Julve, F. Lloret, G. De Munno, W. Wernsdorfer, E. Pardo, *J. Am. Chem. Soc.* **2012**, *134*, 15704; e) S. Mossin, B. L. Tran, D. Adhikari, M. Pink, F. W. Heinemann, J. Sutter, R. K. Szilagyi, K. Meyer, D. J. Mindiola, *J. Am. Chem. Soc.* **2012**, *134*, 13651; f) Y.-Y. Zhu, C. Cui, Y.-Q. Zhang, J.-H. Jia, X. Guo, C. Gao, K. Qian, S.-D. Jiang, B.-W. Wang, Z.-M. Wang, S. Gao, *Chem. Sci.* **2013**, *4*, 1802; g) D. Weismann, Y. Sun, Y. Lan, G. Wolmershäuser, A. K. Powell, H. Sitzmann, *Chem. Eur. J.* **2011**, *17*, 4700; h) J. M. Zadrozny, J. R. Long, *J. Am. Chem. Soc.* **2011**, *133*, 20732; i) J. M. Zadrozny, J. Liu, N. A. Piro, C. J. Chang, S. Hill, J. R. Long, *Chem. Commun.* **2012**, *48*, 3927; j) J. M. Zadrozny, M. Atanasov, A. M. Bryan, C.-Y. Lin, B. D. Rekken, P. P. Power, F. Neese, J. R. Long, *Chem. Sci.* **2013**, *4*, 125.

[5] a) O. Kahn, *Molecular Magnetism*, VCH, Weinheim, **1993**.

[6] a) L. Thomas, L. Lionti, R. Ballou, D. Gatteschi, R. Sessoli, B. Barbara, *Nature* **1996**, *383*, 145; b) G. Christou, D. Gatteschi, D. N. Hendrickson, R. Sessoli, *MRS Bull.* **2000**, *25*, 66; c) M. Murrie, *Chem. Soc. Rev.* **2010**, *39*, 1986.

[7] R. Sessoli, D. Gatteschi, A. Caneschi, M. Novak, *Nature* **1993**, *365*, 149.

[8] a) M. Jeletic, P.-H. Lin, J. J. Le Roy, I. Korobkov, S. I. Gorelsky, M. Murugesu, *J. Am. Chem. Soc.* **2011**, *133*, 19286; b) G.-J. Chen, Y.-N. Guo, J.-L. Tian, J. Tang, W. Gu, X. Liu, S.-P. Yan, P. Cheng, D.-Z. Liao, *Chem. Eur. J.* **2012**, *18*, 2484; c) Y. Wang, X.-L. Li, T.-W. Wang, Y. Song, X.-Z. You, *Inorg. Chem.* **2010**, *49*, 969.

[9] a) P. Gütlich, H. A. Goodwin, *Top. Curr. Chem.* **2004**, *233*, 1; b) X. Bao, P.-H. Guo, W. Liu, J. Tucek, W.-X. Zhang, J.-D. Leng, X.-M. Chen, I. Guralskiy, L. Salmon, A. Bousseksou, M.-L. Tong, *Chem. Sci.* **2012**, *3*, 1629.

[10] A. Bousseksou, G. Molnar, L. Salmon, W. Nicolaz, *Chem. Soc. Rev.* **2011**, *40*, 3313.

[11] E. Goldschmied, N. C. Stephenson, *Acta Crystallogr. Sect. B* **1970**, *26*, 1867.

[12] J. S. Judge, W. A. Baker, Jr., *Inorg. Chim. Acta* **1967**, *1*, 239.

[13] F. E. Mabbs, D. J. Machin, *Magnetism and Transition Metal Complexes*, Dover, Mineola, N.Y., **2008**.

[14] F. Habib, C. Cook, I. Korobkov, M. Murugesu, *Inorg. Chim. Acta* **2012**, *380*, 378.

[15] a) P.-E. Car, M. Perfetti, M. Mannini, A. Favre, A. Caneschi, R. Sessoli, *Chem. Commun.* **2011**, *47*, 3751; b) J. D. Rinehart, K. R. Meihaus, J. R. Long, *J. Am. Chem. Soc.* **2010**, *132*, 7572; c) S.-D. Jiang, B.-W. Wang, H.-L. Sun, Z.-M. Wang, S. Gao, *J. Am. Chem. Soc.* **2011**, *133*, 4730.

[16] a) F. Aquilante, L. De Vico, N. Ferré, G. Ghigo, P.-Å. Malmqvist, P. Neogrády, T. B. Pedersen, M. Pitonák, M. Reiher, B. O. Roos, L. Serrano-Andrés, M. Urban, V. Veryazov, R. Lindh, *J. Comput. Chem.* **2010**, *31*, 224; b) See MOLCAS manual http://www.molcas.org/documentation/manual/node95.html; c) L. F. Chibotaru, L. Ungur, *J. Chem. Phys.* **2012**, *137*, 064112.

[17] A. Abragam, B. Bleaney, *Electron Paramagnetic Resonance of Transition Ions*, Clarendon, Oxford, **1970**.

[18] S. Stoll, A. Schweiger, *J. Magn. Reson.* **2006**, *178*, 42.

  